Pis'ma v ZhETF, vol. 98, iss. 12, pp. 933 – 937

Quantum bicriticality in $Mn_{1-x}Fe_xSi$ solid solutions: exchange and percolation effects

S. V. Demishev[+1)], *I. I. Lobanova*[+*], *V. V. Glushkov*[+*], *T. V. Ischenko*[+], *N. E. Sluchanko*[+], *V. A. Dyadkin*, *N. M. Potapova*, *S. V. Grigoriev*

[+]*A.M.Prokhorov General Physics Institute of the RAS, 119991 Moscow, Russia*

[*]*Moscow Institute of Physics and Technology, 141700 Dolgoprudny, Russia*

Konstantinov Petersburg Nuclear Physics Institute, 188300 Gatchina, Russia

Submitted 8 November 2013

The $T-x$ magnetic phase diagram of $Mn_{1-x}Fe_xSi$ solid solutions is probed by magnetic susceptibility, magnetization and resistivity measurements. The boundary limiting phase with short-range magnetic order (analogue of the chiral liquid) is defined experimentally and described analytically within simple model accounting both classical and quantum magnetic fluctuations together with effects of disorder. It is shown that $Mn_{1-x}Fe_xSi$ system undergoes a sequence of two quantum phase transitions. The first "underlying"quantum critical (QC) point $x^* \sim 0.11$ corresponds to disappearance of the long-range magnetic order. This quantum phase transition is masked by short-range order phase, however, it manifests itself at finite temperatures by crossover between classical and quantum fluctuations, which is predicted and observed in the paramagnetic phase. The second QC point $x_c \sim 0.24$ may have topological nature and corresponds to percolation threshold in the magnetic subsystem of $Mn_{1-x}Fe_xSi$. Above x_c the short-range ordered phase is suppressed and magnetic subsystem becomes separated into spin clusters resulting in observation of the disorder-driven QC Griffiths-type phase characterized by an anomalously divergent magnetic susceptibility $\chi \sim 1/T^{\xi}$ with the exponents $\xi \sim 0.5-0.6$.

DOI: 10.7868/S0370274X13240144

Since mid-eighties it is known that substitution of manganese with iron in $Mn_{1-x}Fe_xSi$ isostructural solid solutions suppresses transition temperature into helical state T_c and leads to disappearance of spontaneous magnetic moment in the range $0.1 < x < 0.2$ [1]. Recent studies revealed that the zero value $T_c(x) = 0$ may be reached for $x^* = 0.12 - 0.15$ [2, 3]. Neutron diffraction experiments showed that rise of x results in decrease of exchange energy, whereas Dzyaloshinskii–Moriya (DM) interaction does not depend on sample composition [2]. The opportunity to satisfy condition $T_c(x^*) = 0$ opens the door to quantum phase transition and observation of the quantum critical (QC) phenomena in $Mn_{1-x}Fe_xSi$. In Ref. [3] authors argue that QC transition in $Mn_{1-x}Fe_xSi$ exists but has "underlying" nature [3]. In practice this statement means that QC point (if any) is located inside some intermediate phase surrounding the $T_c(x)$ line on the magnetic phase diagram. Existence of the intermediate phases of presumably fluctuating nature for $T > T_c(x)$ in $Mn_{1-x}Fe_xSi$ was also reported in [4]. Besides, recent theoretical consideration of the magnetic properties of MnSi within Hubbard model [5] showed that weakening of the on-site repulsion induces transformation of the spiral phase with long-range magnetic order to the partially ordered or fluctuation-driven spiral phase. The considered behavior is very similar to that one caused by chiral condensation effects in quantum helimagnets [6].

The aforementioned theoretical scenarios [5, 6] as well as some experimental results [3] show that QC phenomena in $Mn_{1-x}Fe_xSi$ compounds may be hidden due to formation of the intermediate magnetic phases so that no pronounced anomalies for finite temperatures at QC point (like divergent magnetic susceptibility) should exist. Indeed, no specific effects at $T \neq 0$, which mark unambiguously QC region, have been reported up to now for $Mn_{1-x}Fe_xSi$. From the other hand, the absence of experimentally observed QC anomalies puts into question applicability of any QC model to this system with anisotropic antisymmetric magnetic interactions.

In the present work the $T-x$ magnetic phase diagram of $Mn_{1-x}Fe_xSi$ solid solutions is revisited. We argue that $Mn_{1-x}Fe_xSi$ undergoes a sequence of two quantum phase transitions. In contrast to previous findings,

[1)]e-mail: demis@lt.gpi.ru

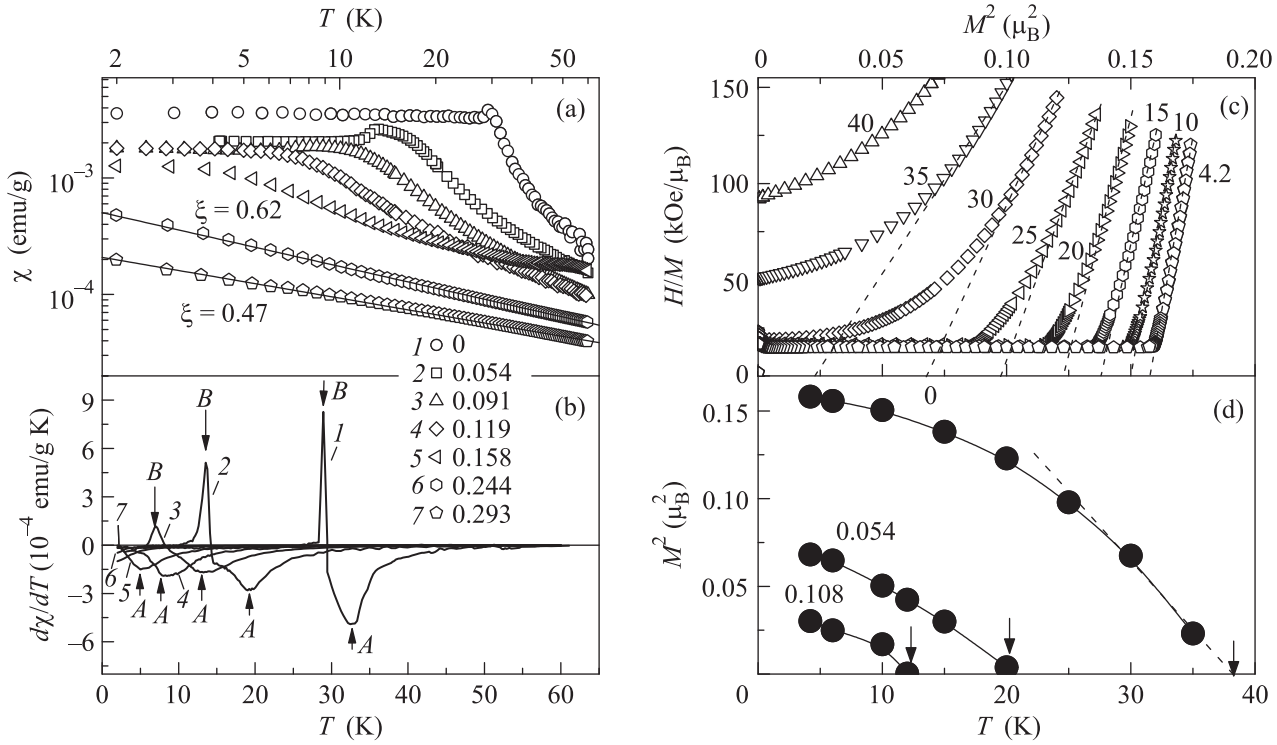

Fig. 1. Magnetic susceptibility (a) and $\partial\chi/\partial T$ (b) in $Mn_{1-x}Fe_xSi$ solid solutions. In the panel (b) peaks A and B correspond to short-range and long-range magnetic ordering, respectively. The legend in the penels (a)–(b) denotes iron concentrations. Arrott plots for MnSi (c) and examples of temperature dependences of the spontaneous magnetization square for $Mn_{1-x}Fe_xSi$ (d). The digits near curves in the panel (c) mark corresponding temperatures

the first underlying QC point $x^* \sim 0.11$ is not completely masked by the intermediate short-ordered phase and manifests itself at finite temperatures by crossover between classical and quantum fluctuations. The second QC point located at $x_c \sim 0.24$ marks onset of the low temperature power divergence of the magnetic susceptibility $\chi \sim 1/T^{\xi}$ and may have a topological nature.

Single crystals of $Mn_{1-x}Fe_xSi$ solid solutions in the range $x < 0.3$ were synthesized by both Czochralski and Bridgeman methods. The quality of the samples was controlled by the X-ray Laue diffraction. As long as real iron content in obtained crystal may differ from nominal x value in initial ingot, all samples were examined by EPMA. Assuming composition formula $(Mn_{1-x}Fe_x)_{1+y}Si_{1-y}$ we find that stoichiometry of crystals keeps at the level $y \sim 0.01-0.005$ comparable with the absolute error of our EPMA measurements. However, the real concentration x in general case was noticeably deviating from the nominal one with discrepancy reaching $\sim 5\%$ of iron content. For that reason the parameters x characterizing studied samples de facto are presented in the following consideration. The third digit in the x number below is used as a reference and corresponds to average Fe content obtained by several scans along the sample surface. It is worth noting that in the previous studies [2–4] authors referred to the nominal iron concentration, which may distort the shape of magnetic phase diagram. The magnetization and magnetic susceptibility data in magnetic field up to 5 T were obtained with a SQUID magnetometer (Quantum Design). The resistivity data $\rho(T)$ were measured by standard DC four probe technique at temperatures 1.8 – 300 K.

Temperature dependences of the magnetic susceptibility in $Mn_{1-x}Fe_xSi$ show clearly (Fig. 1a) that for iron content exceeding $x_c \sim 0.24$ the $\chi(T)$ data follow power law $\chi \sim 1/T^{\xi}$ with the exponent $\xi < 1$. The parameter ξ tends to decrease with x from $\xi = 0.62 \pm 0.02$ ($x = 0.244$) to $\xi = 0.47 \pm 0.01$ ($x = 0.293$). This type of anomaly is typical for QC behavior and therefore it is necessary to examine the $T-x$ magnetic phase diagram in more detail for checking this supposition. In order to reconstruct magnetic phase diagram from magnetic measurements it is possible to consider two various options. Detailed comparison of the $\partial\chi/\partial T = f(T)$ curves with the magnetic structure data carried in [4] shows that broad minima A on the $\partial\chi/\partial T$ temperature dependences (Fig. 1b) correspond to formation of an inter-

mediate phase, whereas narrow peaks B reflect the onset of the helical phase with long-range magnetic order. Note that for the concentrations exceeding $x^* = 0.108$ peak B disappears while minimum A still exists up to x_c. For $x > x_c = 0.24$ the A minimum is not observed in the studied range of experimental parameters (Fig. 1b). Another opportunity is based on the application of the classical ferromagnetic equation of state to the case of $Mn_{1-x}Fe_xSi$ [3] that results in Arrott plot procedure (Fig. 1c) with subsequent standard extrapolation of spontaneous magnetization square $M^2 = f(T)$ to the value $M = 0$ (Fig. 1d).

In addition to this extrapolation procedure expected in Landau theory (Fig. 1d) the plot $M^2 = f(T^2)$ suggested in [3] was also examined. Both methods provide almost the same characteristic temperatures and therefore we will restrict ourselves below by the results of the standard approach. It is interesting that Arrott analysis gives transition temperatures which lie well above T_c even for $x = 0$, i.e. in pure MnSi (compare Figs. 1b and d).

All aforementioned results are summarized in Fig. 2 where various transition points $T_s(x)$ are plotted on the

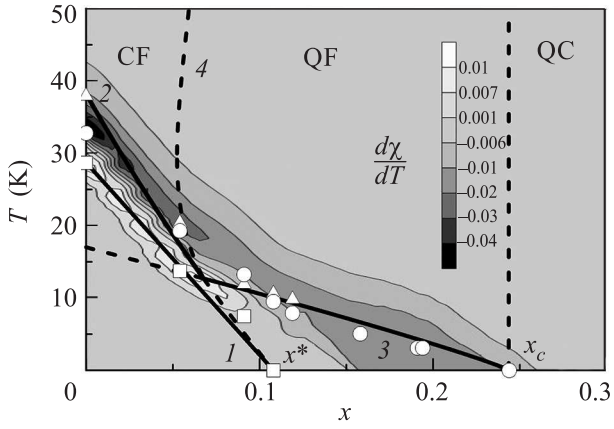

Fig. 2. The map of $\partial\chi/\partial T$ and $T - x$ magnetic phase diagram. Squares denote transition into the phase with long-range magnetic order; triangles and circles represent results of Arrott plot and $\partial\chi/\partial T$ analysis accordingly. The lines *1–4* correspond to the analytical model (see text for details)

background of the $\partial\chi/\partial T = f(x, T)$ map. Temperatures obtained from $\partial\chi/\partial T$ minima (circles) and Arrott plots (triangles) coincidence reasonably for $x \geqslant 0.05$, whereas for $x = 0$ Arrott analysis gives $T_s(x = 0)$ close to the inflection point of the susceptibility derivative. In general case the transitions $T_s(x)$ mark broad $\partial\chi/\partial T$ feature preceding formation of the long range magnetic order at $T_c(x)$ (lines B in Fig. 1 and squares in Fig. 2). As long as ferromagnetism appears at $T_s > T_c$ it is natural to interpret T_s as a transition temperature into phase with short-range magnetic order, which has chiral character as suggested by structural data [4]. Interestingly, although exchange interaction is expected to turn to zero at the same point x^* as $T_c(x)$ [2] the phase with short range order (chiral liquid in terminology of [6]) exists up to $x_c > x^*$ (Fig. 2).

The results obtained suggest a new scenario of quantum criticality in $Mn_{1-x}Fe_xSi$. There are two QC transitions at $T = 0$: the first one corresponds to transition between long-range and short range ordered phase at x^*, whereas the second one is located at $x_c > x^*$ and separates the phase with short-range magnetic order and QC phase with the power divergence of magnetic susceptibility (Fig. 2). The QC anomalies at finite temperatures may be observed only above x_c when any types of detectable magnetic order are suppressed because these anomalies are masked by effects of short-range ordering at "underlying" point x^* (Figs. 1 and 2). The considered quantum *bicritical* behavior is very unusual and thus doubly suffers from the statement that magnetic phase diagram in Fig. 2 is reconstructed from finite (and rather high) temperature experiments and therefore extrapolation to zero temperature does not seem to be correct. For elucidating the quantum bicritical scenario and proving x_c as a real QC boundary the simple phenomenological model is proposed below.

We assume that short-range magnetic order phase in $Mn_{1-x}Fe_xSi$ (chiral liquid [6]) develops when fluctuations of the order parameter in the paramagnetic phase (chiral gas [6]) slow down and freeze. When $T \to T_c(x)$ the radius of classical fluctuations R_{f1} increases and short-range order for $x > x^*$ appears when R_{f1} reaches some critical value. As temperature of the transition into the phase with long-range magnetic order for $x > x^*$ becomes zero, $T_c(x) \equiv 0$, the same supposition could be applied to the case of quantum fluctuations [7]. The conditions of freezing may be expressed as $R_{f1,2} = R_s$, where $R_{f1,2}$ are spatial scales of fluctuations, and R_s denotes some characteristic length in the considered material (the idea of comparison of the characteristic length scales for magnetic phase transitions in MnSi was earlier introduced in [8]). The considered phase transitions in $Mn_{1-x}Fe_xSi$ are expected to be driven by disorder effects in the magnetic subsystem, which may be taken into account in the considered model assuming that R_s is given by correlation length R_c of the infinite percolation cluster [9]

$$R_s = R_c(x) = \frac{l}{(1 - x/x_c)^{\nu}}. \qquad (1)$$

In Eq. (1) l is the minimal length about unit cell size relevant to the ordered case ($x = 0$), x_c is a percolation threshold, and $\nu = 0.9$ [9].

Using standard expressions for classical and quantum fluctuations [7]

$$R_{f1} = \frac{a_1}{(T/T_c - 1)^{\delta}}; \quad R_{f2} = a_2 \frac{T_0}{T} \tag{2}$$

we compute temperatures of the transitions into the phase with short-range order:

$$\begin{aligned} T_1(x) &= T_c(x) \left[1 + \frac{\delta T(0)}{T_c(0)} \left(1 - \frac{x}{x_c} \right)^{\nu/\delta} \right]; \\ T_2(x) &= T_2(0) \left(1 - \frac{x}{x_c} \right)^{\nu}. \end{aligned} \tag{3}$$

Hereafter indexes "1" and "2" denotes classical and quantum cases respectively. In Eqs. (2), (3) $\delta T(0) = T_1(0) - T_c(0) = (a_1/l)^{1/\delta} T_c(0)$ is the temperature range of the intermediate phase preceding long-range ordering at $x = 0$ and $T_2(0) = (a_2/l)T_0$. The parameters $a_{1,2}$ have dimension of length and T_0 stands for the energy scale defining quantum fluctuations [7].

In the standard theory of QC phenomena the characteristic concentrations x^* and x_c coincide [7] and thus accounting of these two types of fluctuations results in possible renormalization of the fluctuation region around T_c. A new type of the magnetic phase diagram appears in the considered bicritical case when $x^* \neq x_c$ and $x^* < x_c$. The temperature $T_2(x)$ gives a short-range order "tail" above x^*, which disappears at the second quantum critical point x_c in qualitative agreement with experimentally observed behavior (Fig. 2).

In further calculations a linear approximation $T_c(x) = T_c(0)(1 - x/x^*)$ for the transition temperature into the phase with long-range magnetic order (chiral solid of [6]) will be used (line *1* in Fig. 2). The parameters $\delta T(0)$, x^* and x_c are known from experiment and if the value of the critical exponent δ is fixed the approximation of experimental data with Eqs. (3) reduces to a computation with the single free parameter $T_2(0)$. The best fit results obtained for $\delta = 1/2$ and $T_2(0) = 17$ K are shown in Fig. 2 by line *2* denoting $T_1(x)$ and line *3* representing $T_2(x)$. It is visible that the proposed model allows reasonably describe magnetic phase diagram of $Mn_{1-x}Fe_xSi$ supporting the suggested quantum bicritical scenario.

It is interesting that the obtained $T_2(0)$ value is very close to the position of the low temperature anomaly at ~ 15 K discovered recently from the study of the magnetoresistance and electron spin resonance for pure MnSi [10, 11]. Within the proposed model this feature may be linked to the quantum fluctuations effects, i.e. dashed section of the line *3* in Fig. 2 is expected to correspond to a real line on the magnetic phase diagram inside chiral solid. It is worth noting that up to now the characteristic point $T \sim 15$ K in MnSi had no interpretation. The considered supposition implies possible co-existence of the classical and quantum fluctuations below x^* suggesting a new phenomenon potentially observable in the paramagnetic phase. The condition $R_{f1}(T, x) = R_{f2}(T)$ defines the line $T_{eq}(x)$, which can be computed without introduction of any additional fitting parameters from the equation

$$A = z^2/(z - 1), \tag{4}$$

where $z = T_{eq}(x)/T_c(x)$ and $A = T_2(0)^2/\delta T(0) T_c(x)$. The result is shown by dashed line *4* in Fig. 2. To the left from the $T_{eq}(x)$ the classical fluctuations dominate (the region CF in Fig. 2) and to the right from the $T_{eq}(x)$ the quantum fluctuations rule the paramagnetic phase (the region QF in Fig. 2).

The $\partial\chi/\partial T$ data do not show any presence of the expected $T_{eq}(x)$ (Fig. 2). However the situation changes for the temperature dependences of the resistivity $\rho(T)$. The experimental $\rho(T)$ curves for various $Mn_{1-x}Fe_xSi$ samples were fitted by the expression $\rho(T) = \rho(0) + AT^{\alpha}$ and the values of the exponent $\alpha(x, T)$ were used to draw $\alpha(x, T)$ map. The result together with the magnetic phase diagram lines obtained above is plotted in Fig. 3. It is remarkable that apart from the peculiarities observed in the vicinity of the quantum critical points at x^* and x_c as well as around $T_c(0)$ and low temperature anomaly $T_2(0)$ the predicted crossover region between classical and quantum fluctuations is clearly marked by broad minima of $\alpha(x, T)$ (Fig. 3). Thus the

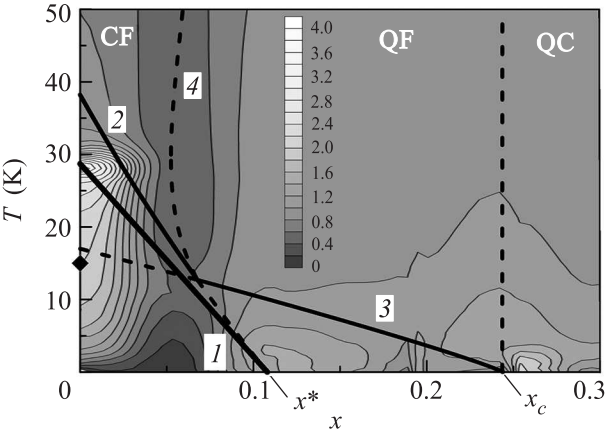

Fig. 3. The map of the exponent $\alpha(x, T)$ in the temperature dependences of resistivity and magnetic phase diagram obtained from magnetic measurements

$T_{eq}(x)$ line expected from the analysis of the *magnetic measurements* is detected in the *resistivity* data. In order to explain this behavior, first of all, it is necessary to take into account that the $\partial\chi/\partial T$ map corresponds to the averaged picture, which is not affected by fluctuations unless they freeze out. The case of resistivity is different. Recent investigation showed that magnetic scattering dominates in transport properties of MnSi [11] and hence scattering on magnetic fluctuations will affect resistivity data. Thus the visualization of a new line dividing classical and quantum fluctuations just in $\alpha(x,T)$ gets natural explanation.

At present, magnetic properties of MnSi-based compound could be understood either within itinerant models or within a model of the Heisenberg-type localized magnetic moments [10, 11]. In the former case, the reason for suppression of the long-range magnetic order at x^* is a decrease of on-site Hubbard repulsion [5]. In Heisenberg-type models [2–4, 10–12] the transition between chiral solid and chiral liquid states may be caused by competition between frustration expected for RKKY interaction, which orient spin spirals along (110) axis [12], whereas DM interaction favors (111) direction [2, 4]. Under this assumption it is also possible to suppose that classical fluctuations are mainly driven by exchange interaction, while quantum fluctuations may originate from DM interaction and thus could exist in the whole concentration range [2].

The suggested percolation description of the magnetic phase diagram for $x > x^*$ means that bounding of the $Mn_{1-x}Fe_xSi$ magnetic subsystem breaks at the percolation threshold and for $x > x_c$ the magnetic subsystem should consist of separate spin clusters. Consequently, it is reasonable to expect that the observed QC phase (region QC in Figs. 2, 3) is nothing but Griffiths phase [13, 14]. The experimental values of the magnetic susceptibility critical exponents $\xi \sim 0.5-0.6$ (Fig. 1) are close to those ones expected in the mean-field approximation [15] and hence the aforementioned supposition at least does not contradict the experimental data.

In conclusion, the combination of magnetic susceptibility and resistivity data together with the proposed model strongly supports suggested quantum bicritical $T-x$ magnetic phase diagram of $Mn_{1-x}Fe_xSi$. The "underlying" QC point $x^* \sim 0.11$, although being masked by short-range order phase, manifests itself by the crossover between classical and quantum fluctuations, which is predicted and observed experimentally in the paramagnetic phase. The second quantum critical point $x_c \sim 0.24$ may have topological nature and corresponds to percolation threshold in the magnetic subsystem of $Mn_{1-x}Fe_xSi$. Above x_c the transition into the short-range ordered phase is suppressed and magnetic subsystem becomes separated into spin clusters resulting in the disorder-driven QC phase with anomalously divergent magnetic susceptibility.

This work was supported by Programme of Russian Academy of Sciences "Strongly correlated electrons" and by RFBR grant # 13-02-00160.

1. Y. Nishihara, S. Waki, and S. Ogawa, Phys. Rev. B **30**, 32 (1984).
2. S. V. Grigoriev, V. A. Dyadkin, E. V. Moskvin, D. Lamago, Th. Wolf, H. Eckerlebe, and S. V. Maleyev, Phys. Rev. B **79**, 144417 (2009).
3. A. Bauer, A. Neubauer, C. Franz, W. Münzer, M. Garst, and C. Pfleiderer, Phys. Rev. B **82**, 064404 (2010).
4. S. V. Grigoriev, E. V. Moskvin, V. A. Dyadkin, D. Lamago, Th. Wolf, H. Eckerlebe, and S. V. Maleyev, Phys. Rev. B **83**, 224411 (2011).
5. F. Kruger, U. Karahasanovic, and A. G. Green, Phys. Rev. Lett. **108**, 067003 (2012).
6. S. Tewari, D. Belitz, and T. R. Kirkpatrick, Phys. Rev. Lett. **96**, 047207 (2006).
7. S. Sachdev, *Quantum phase transitions*, 2th ed., Cambridge University Press (2011).
8. T. Vojta and R. Sknepnek, Phys. Rev. B **64**, 052404 (2001).
9. A. L. Efros, *Physics and Geometry of Disorder: Percolation Theory*, Mir Publishers (1986).
10. S. V. Demishev, A. V. Semeno, A. V. Bogach, V. V. Glushkov, N. E. Sluchanko, N. A. Samarin, and A. L. Chernobrovkin, JETP Lett. **93**, 213 (2011).
11. S. V. Demishev, V. V. Glushkov, I. I. Lobanova, M. A. Anisimov, V. Yu. Ivanov, T. V. Ishchenko, M. S. Karasev, N. A. Samarin, N. E. Sluchanko, V. M. Zimin, and A. V. Semeno, Phys. Rev. B **85**, 045131 (2012).
12. J. M. Hopkinson and H. Y. Kee, Phys. Rev. B **75**, 064430 (2007).
13. R. B. Griffiths, Phys. Rev. Lett. **23**, 17 (1969).
14. A. J. Bray, Phys. Rev. Lett. **59**, 586 (1987).
15. D. Belitz, T. R. Kirkpatrick, and J. Rollbuhler, Phys. Rev. Lett. **94**, 247205 (2005).